Processing and Application of Ceramics 12 [3] (2018) 257–261
https://doi.org/10.2298/PAC1803257W

Facile molten salt synthesis of zirconia whiskers

Tao Wang[1], Jianmin Liu[2], Weihui Jiang[1,2,*], Guo Feng[2], Lifeng Miao[2], Ting Chen[2], Qian Wu[2], Huidong Tang[1], Wei Luo[1]

[1]*School of Material Science and Engineering, Jingdezhen Ceramic Institute, Jingdezhen, Jiangxi 333403, China*
[2]*National Engineering Research Center for Domestic and Building Ceramics, Jingdezhen, Jiangxi 333001, China*

Received 17 April 2018; Received in revised form 22 July 2018; Accepted 17 August 2018

Abstract

ZrO_2 whiskers have been synthesized by a facile molten salt method using $ZrOCl_2 \cdot 8\,H_2O$ and $Na_3PO_4 \cdot 12\,H_2O$ as the zirconium source and molten salt, respectively. Differential thermal and thermogravimetric analyses, X-ray diffraction analysis, field emission scanning electron microscope and transmission electron microscope were employed to characterize the heating process of the precursor mixture, phase composition of the as-synthesized ZrO_2 whiskers and the effect of reaction temperature on the synthesis of ZrO_2 whiskers. The results show that the ZrO_2 whiskers synthesized at 900 °C have an average aspect ratio of 30 and preferentially grow along [010] direction. The formation of sodium zirconium phosphate [$Na_{9-4x}Zr_x(PO_4)_3$] (x = 1, 2) and the reaction temperature play an important role in the growth of ZrO_2 whiskers. This work also suggests an effective route for mass production of high quality ZrO_2 whiskers.

Keywords: *molten salt method, zirconia whisker, crystal growth, sodium zirconium phosphate*

I. Introduction

Zirconia has been extensively studied in high-temperature structural materials, ceramic tools, bioceramics, solid fuel cells, oxygen sensors and catalytic materials due to its valuable physical and chemical properties, such as high melting point, high resistance to thermal shock, low thermal and electrical conductivity, excellent wear resistance, and biocompatibility [1–3]. Whisker is a kind of fibrous single crystal and has theoretical strength close to perfect crystal owing to its highly complete internal and external structure [4]. In view of the merits of ZrO_2 and whisker, ZrO_2 whisker will show broad prospects in reinforcing and toughening areas, especially for ceramic materials, since they are often quite brittle, limiting their applications in some instances. In addition, zirconia whisker is also expected to be applied in improving sensitivity of chemical sensors due to its high aspect ratio and small size [5].

Up to now, preparation methods for ZrO_2 whiskers are mainly focused on high pressure and high temperature method [6], chemical vapour deposition (CVD) method [7,8], and hydrothermal method [9,10]. Compared with the strict preparation conditions or long experimental period in above methods, molten salt method has been developed as a promising route for preparation of ZrO_2 whiskers [11], but the complex preparation process of precursor and the low aspect ratio (about 18) limit its further application. Molten salt method is reported to be one of the simplest methods and widely used in the synthesis of powders [12], nanorods [13], whiskers [14] and other materials due to its excellent molten salt flux in favour of crystal growth [15].

For typical molten salt synthesis, in this work we developed a novel ZrO_2 whiskers preparation strategy by means of using raw materials without pretreatment. The as-synthesized ZrO_2 whiskers showed an improved quality. The effect of reaction temperature on the synthesis of ZrO_2 whiskers is systematically investigated and the formation mechanism of ZrO_2 whiskers is also discussed.

II. Experimental

Analytically pure $ZrOCl_2 \cdot 8\,H_2O$, $Na_3PO_4 \cdot 12\,H_2O$ and NaF were used as starting materials. The powders

*Corresponding authors: tel: +86 798 8499328, e-mail: *whj@jci.edu.cn*

of 2 g $ZrOCl_2 \cdot 8\,H_2O$, 2 g $Na_3PO_4 \cdot 12\,H_2O$ and 0.2 g NaF were weighed and mixed. After being ground homogeneously, the precursor mixture was transferred into a corundum crucible and calcined at different temperatures for 5 h, then cooled down to room temperature. The product was washed 3 times with deionized water to remove residual salt and dried at 70 °C for 6 h.

The DTA-TG analysis of the precursor mixture was performed by NETZSCH STA449C (air atmosphere, heating rate: 10 °C/min). The phase composition of the as-synthesized samples was studied by XRD (Bruker D8 Advance). The morphology of ZrO_2 whiskers was observed by FE-SEM (SU8010) and TEM (JEM-2010). Crystal structure and growth direction of ZrO_2 whiskers were characterized by SAED and HR-TEM.

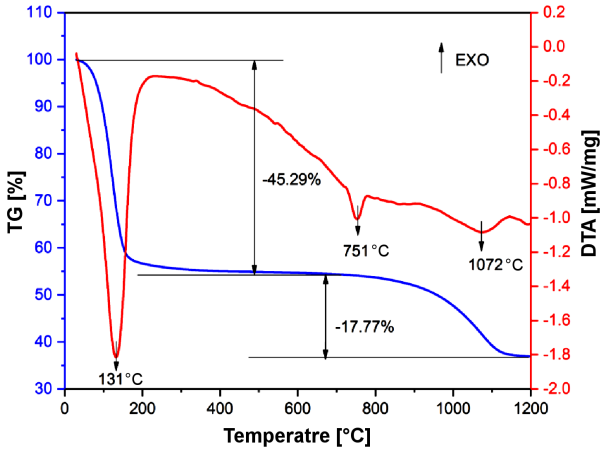

Figure 1. DTA-TG curve of the mixed precursors ($ZrOCl_2 \cdot 8\,H_2O$, $Na_3PO_4 \cdot 12\,H_2O$ and NaF)

III. Results and discussion

Figure 1 shows the DTA-TG curves of the precursor mixture. In the TG curve two obvious stages can be observed in temperature ranges of 20–500 °C and 820–1170 °C. The first weight loss is about 45.29% and can be divided into two parts. The part one is from room temperature to 230 °C, which is the main weight loss part caused by the evaporation of crystalline water present in $Na_3PO_4 \cdot 12\,H_2O$ [16] and $ZrOCl_2 \cdot 8\,H_2O$ [17]. The part two is from 230 to 500 °C, which is due to the volatilization of HCl produced by the transformation of dehydrated $ZrOCl_2$ to ZrO_2 [17]. The second weight loss is about 17.77%, corresponding to the volatilization of molten salt. In the DTA curve, a sharp endothermic peak at 131 °C can be attributed to the evaporation of crystalline water. The endothermic peak at 751 °C is caused by the formation of liquid molten salt, confirmed by no obvious weight loss in TG curve. The broad endothermic peak from 820 to 1170 °C is due to the volatilization of molten salt.

The phase composition of the as-synthesized samples prepared at different temperatures is examined by XRD (Fig. 2). Only tetragonal zirconia (t-ZrO_2) appears at 300 °C and the broad diffraction peak demonstrates a poor crystallinity and tiny size of the obtained sample. Not only diffraction peaks of t-ZrO_2 and small amount of monoclinic zirconia (m-ZrO_2), but $Na_2Zr(PO_4)_2$ and $NaZr_2(PO_4)_3$ are observed at 500 °C. The occurrence of t-ZrO_2 at room temperature is due to the crystallite size effect (below 30 nm). The increased grain size will lead to the phase transformation of t-ZrO_2 to m-ZrO_2 with the increase of heat treatment temperature [18]. The phase of $Na_2Zr(PO_4)_2$ and $NaZr_2(PO_4)_3$ can be classified as sodium zirconium phosphates, $Na_{9-4x}Zr_x(PO_4)_3$

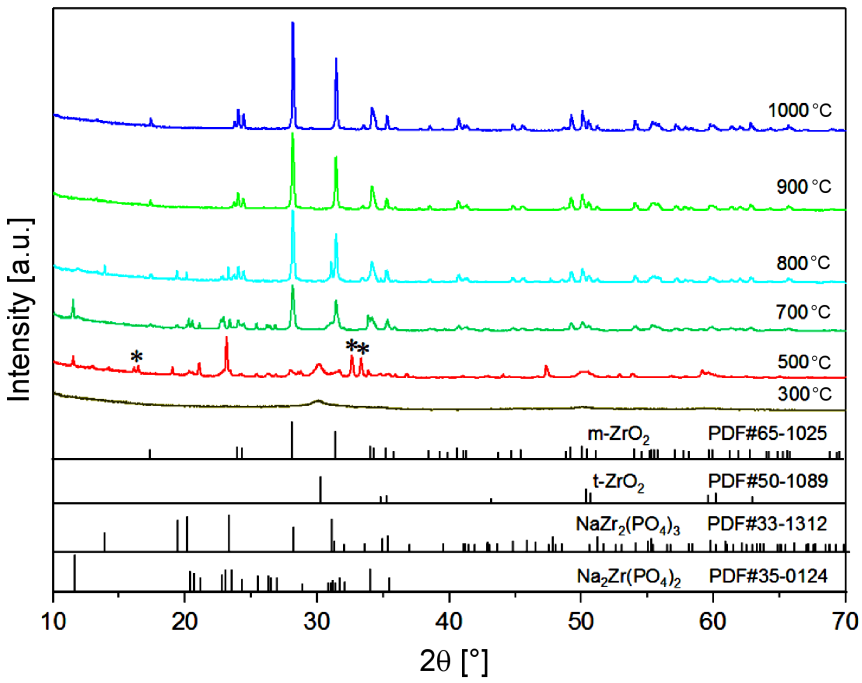

Figure 2. XRD patterns of as-synthesized samples prepared at different temperatures (* unknown diffraction peaks)

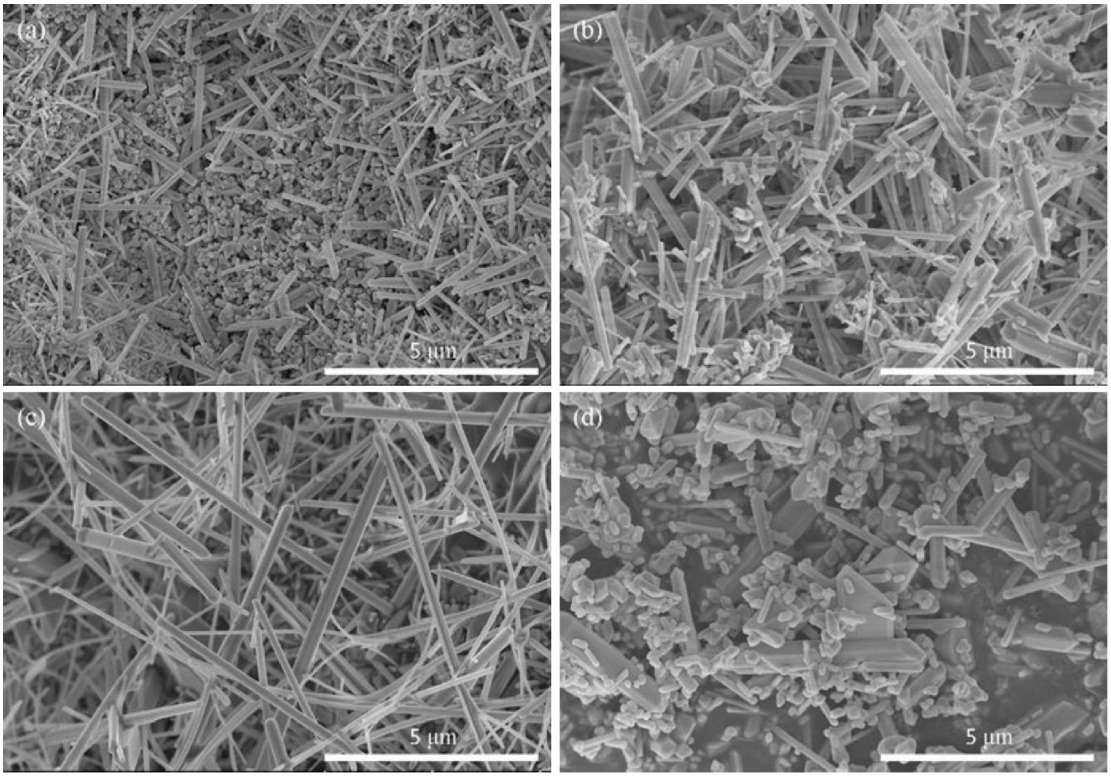

Figure 3. FE-SEM micrographs of samples synthesized at different temperatures: a) 700, b) 800, c) 900 and d) 1000 °C

(x = 1, 2), which shows an extensive solid solution of ZrO_2 in Na_3PO_4 [19]. Diffraction peaks of m-ZrO_2 and $Na_{9-4x}Zr_x(PO_4)_3$ (x = 1, 2) are detected at 700 and 800 °C. As the temperature rises to 900 and 1000 °C, only m-ZrO_2 is present and no secondary phase is observed, indicating that $Na_{9-4x}Zr_x(PO_4)_3$ will dissolve in liquid molten salt and release ZrO_2 at high temperature. The whole process can be divided into following three stages: i) the decomposition of $ZrOCl_2 \cdot 8\,H_2O$ (equation 1); ii) the formation of $Na_{9-4x}Zr_x(PO_4)_3$ (x = 1, 2) (equation 2); iii) the release of ZrO_2 from $Na_{9-4x}Zr_x(PO_4)_3$ (equation 3).

$$ZrOCl_2 \cdot 8\,H_2O \longrightarrow ZrO_2 + 7\,H_2O + 2\,HCl \quad (1)$$

$$xZrO_2 + 3\,Na_3PO_4 \cdot 12\,H_2O \longrightarrow Na_{9-4x}Zr_x(PO_4)_3 + 12\,H_2O \quad (2)$$

$$Na_{9-4x}Zr_x(PO_4)_3 \longrightarrow xZrO_2 + 3\,Na_3PO_4 \quad (3)$$

FE-SEM micrographs of the samples synthesized at different temperatures are presented in Fig. 3. When the reaction is carried out at 700 °C (Fig. 3a), the sample is made of particles and tiny bars. Compared with the short ZrO_2 whiskers obtained at 800 °C (Fig. 3b) and the stumpy ZrO_2 whiskers obtained at 1000 °C (Fig. 3d), ZrO_2 whiskers synthesized at 900 °C (Fig. 3c) show better quality and have an average aspect ratio of 30, which is comparable with the aspect ratio of ZrO_2 whiskers synthesized by chemical vapour deposition [8].

Low-magnification FE-SEM micrograph of ZrO_2 whiskers prepared at 900 °C is shown in Fig. 4a. Well dispersed ZrO_2 whiskers with 100–250 nm in diameter have a uniform length ranging from 4 μm to 6 μm. The TEM image (Fig. 4b) reveals that the as-synthesized ZrO_2 whisker presents a flat and smooth surface. Three legible spots in the SAED pattern (Fig. 4c) are indexed as (101), (010) and (111) planes (PDF#65-1025) and the zone axis of the SAED is in [01] direction, which indicates the single crystalline nature of the ZrO_2 whisker. The HR-TEM image (Fig. 4d) corresponding to SAED pattern shows the lattice fringe of 0.528 nm, which is in good agreement with the (010) lattice spacing of the m-ZrO_2. It can be concluded from above results that the ZrO_2 whisker preferentially grows along [010] direction.

The reaction temperature has a great influence on the preparation of ZrO_2 whiskers. When the reaction temperature is 700 °C, the molten salt has not been melted completely or it is too viscous to flow, thus it cannot take the role of flux and effectively promote the one dimensional crystal growth. Although the molten salt has been melted at 800 °C, the negligible volatilization of molten salt (Fig. 1) and the incomplete dissolution of $NaZr_2(PO_4)_3$ (Fig. 2) result in the significantly low supersaturation, which is not beneficial for the growth of ZrO_2 whiskers. In comparison, a little volatilization of molten salt (Fig. 1) and the complete dissolution of $NaZr_2(PO_4)_3$ (Fig. 2) at 900 °C lead to the proper supersaturation, which is favourable for the one dimensional preferential growth of zirconia whiskers [20]. In addition, the excessive volatilization of molten salt at 1000 °C (Fig. 1) causes too high supersaturation, which is not beneficial for the preparation of high quality zirconia whiskers.

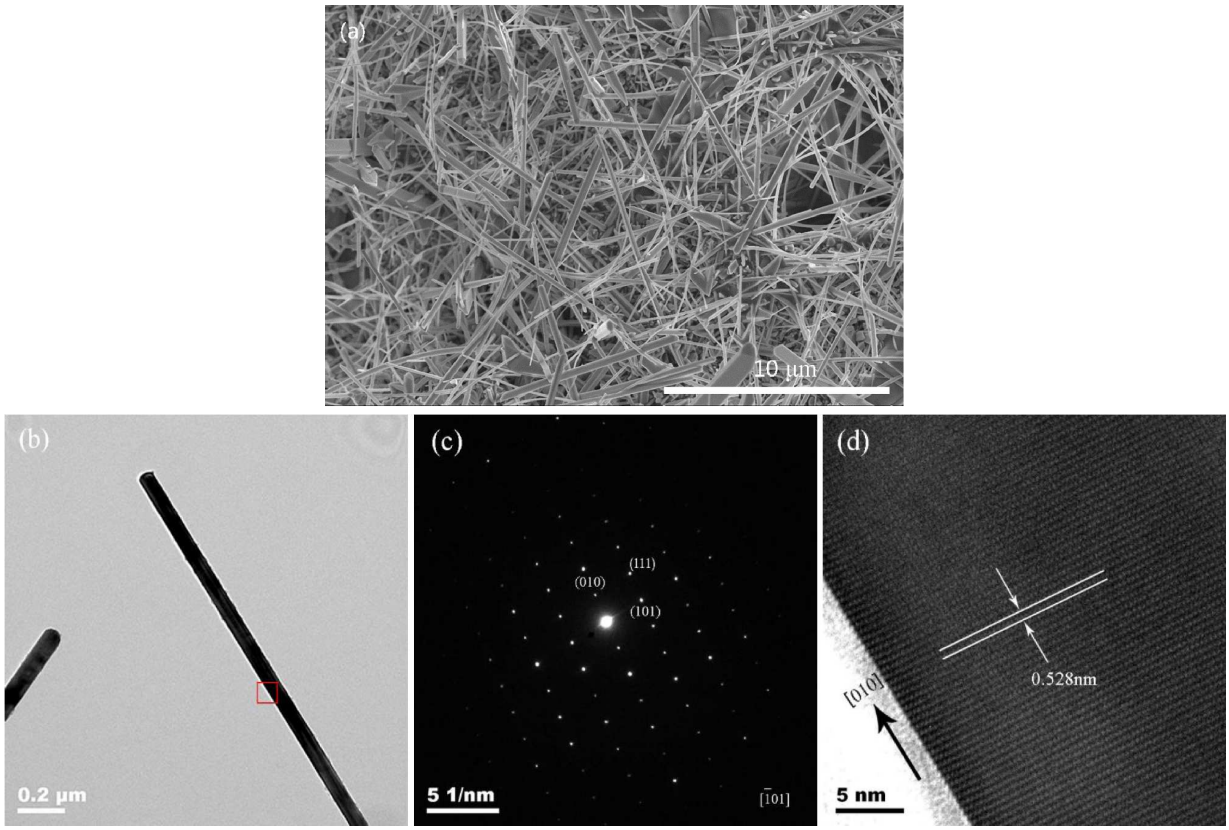

Figure 4. FE-SEM micrograph (a), TEM image (b), SAED pattern (c) and HR-TEM image (d) of ZrO_2 whiskers synthesized at 900 °C

A schematic diagram of the growth mode is presented in Fig. 5. Most of the reactions in salt medium generally follow nucleation and growth process of an oxide compound through the dissolution of precursors and precipitation of oxide product [21]. The first step is key for the following crystal growth and it is usually difficult to find a proper molten salt for the dissolution of precursor, especially for ZrO_2. In this work, $ZrOCl_2 \cdot 8\,H_2O$ and $Na_3PO_4 \cdot 12\,H_2O$ are used as the precursor and molten salt, respectively. During the heating process, $ZrOCl_2 \cdot 8\,H_2O$ is first converted into ZrO_2 and exists in t-ZrO_2 due to the size effect (Fig. 5a) [18]. Then $Na_{9-4x}Zr_x(PO_4)_3$ (x = 1, 2) is formed by the solid reaction between small amount of ZrO_2 and $Na_3PO_4 \cdot 12\,H_2O$ (Fig. 5b). Afterwards, the release of ZrO_2 from the dissolved $Na_{9-4x}Zr_x(PO_4)_3$, combined with the volatilization of molten salt, leads to the supersaturation of ZrO_2 in liquid molten salt. From then on, the supersaturation fosters the precipitation and one dimensional growth of ZrO_2 on the surface of undissolved zirconia nuclei (Fig. 5c). Finally, the ZrO_2 grows into high quality ZrO_2 whiskers (Fig. 5d).

IV. Conclusions

In this work we developed a facile molten salt method to prepare ZrO_2 whiskers. The DTA-TG analysis reveals the melting and volatilization temperature of molten

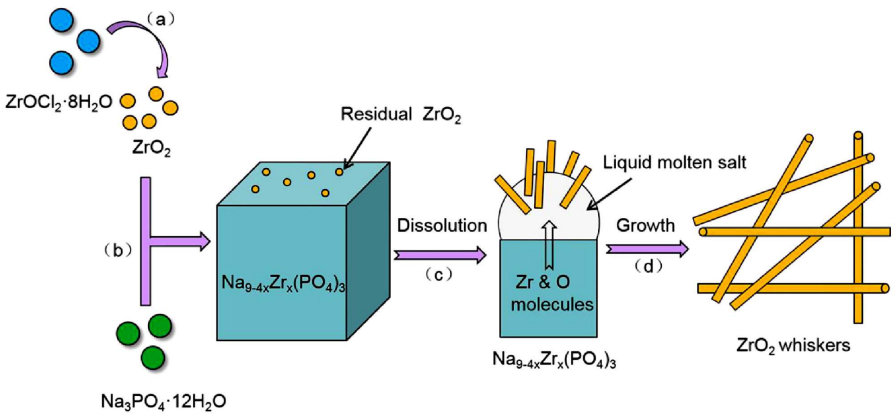

Figure 5. A schematic diagram of the nanostructure growth process

salt. The XRD results show that the sodium zirconium phosphate $Na_{9-4x}Zr_x(PO_4)_3$ (x = 1, 2) is formed at low temperature and gradually disappears with the elevating temperature. The DTA-TG analysis combined with XRD results is in good agreement with the morphology changes presented in FE-SEM micrographs. The ZrO_2 whiskers synthesized at 900 °C have an uniform length ranging from 4 μm to 6 μm with average aspect ratio of 30 and preferential growth along [010] direction. The reaction temperature and the formation of $Na_{9-4x}Zr_x(PO_4)_3$ (x = 1, 2) is favourable for the growth of ZrO_2 whiskers by adjusting the dissolution and precipitation of ZrO_2. Furthermore, this work suggests a valuable way for mass production of high quality ZrO_2 whiskers.

Acknowledgement: The authors are grateful for the Fund for National Natural Science Foundation of China (51662016), the Fund for Distinguished Young Scholars of Jiangxi Province (20171BCB23071), the Fund for Science Foundation of Jiangxi Province (GJJ160881).

References

1. L. Kumari, W. Z. Li, J.M. Xu, R.M. Leblanc, D.Z. Wang, Y. Li, H. Guo, J. Zhang, "Controlled hydrothermal synthesis of zirconium oxide nanostructures and their optical properties", *Cryst. Growth Des.*, **9** [9] (2009) 3874–3880.
2. C. Piconi, G. Maccauro, "Zirconia as a ceramic biomaterial", *Biomaterials*, **20** [1] (1999) 1–25.
3. J.L. Gole, S.M. Prokes, J.D. Stout, O.J. Glembocki, R. Yang, "Unique properties of selectively formed zirconia nanostructures", *Adv. Mater.*, **18** [5] (2010) 664–667.
4. W. Li, Z.L. Jin, Z.H. Zhang, "Application and synthesis of inorganic whisker materials", *Prog. Chem.*, **15** [4] (2003) 264–274.
5. W.S. Dong, F.Q. Lin, C.L. Liu, M.Y. Li, "Synthesis of ZrO_2 nanowires by ionic-liquid route", *J. Colloid Interface Sci.*, **333** [2] (2009) 734–740.
6. C. Xu, D.W. He, C. Liu, H. Wang, P. Wang, Q. Wang, W. Wang, "Preparation of ZrO_2 whiskers through high pressure and high temperature method", *Solid State Sci.*, **41** (2015) 52–55.
7. M. Egashira, H. Katsuki, S. Takatsuki, "Vapor phase growth of monoclinic ZrO_2 whiskers", *Int. J. High Technol. Ceram.*, **3** [4] (1987) 335–335.
8. M.K. Baek, S.J. Park, D.J. Choi, "Synthesis of zirconia (ZrO_2) nanowires via chemical vapor deposition", *J. Cryst. Growth*, **459** (2017) 198–202.
9. Y. Murase, E. Kato, "Preparation of zirconia whiskers from zirconium hydroxide in sulfuric acid solutions under hydrothermal conditions at 200 °C", *J. Am. Ceram. Soc.*, **84** [11] (2010) 2705–2706.
10. E. Kato, A. Nagai, M. Hirano, Y. Kobayashi, "Growth of whiskered ZrO_2 crystals by hydrothermal decomposition of zirconium oxide sulphate pseudo-crystals", *J. Mater. Sci.*, **32** [7] (1997) 1789–1794.
11. J.M. Liu, Q.W. Gao, W.H. Jiang, G. Feng, T. Chen, L.F. Miao, "Preparation of zirconia whiskers", *J. Chin. Ceram. Soc.*, **45** [7] (2017) 984–989.
12. J.F. Ni, H.H. Zhou, J.-T. Chen, X.-X. Zhang, "Molten salt synthesis and electrochemical properties of spherical $LiFePO_4$ particles", *Mater. Lett.*, **61** [4-5] (2007) 1260–1264.
13. A.N. Baranov, G.N. Panin, T.W. Kang, Y.-J. Oh, "Growth of ZnO nanorods from a salt mixture", *Nanotechnology*, **16** [9] (2005) 1918.
14. A. Cuneyt Tas, "Molten salt synthesis of calcium hydroxyapatite whiskers", *J. Am. Ceram. Soc.*, **84** [2] (2001) 295–300.
15. G. Ji, X.H. Lin, Y.Y. Sun, S.A.A. Trimizi, H. Su, Y. Du, "Molten salt growth and magnetic properties of octahedral $CoFe_2O_4$ crystals: Effects of synthesis conditions", *Cryst. Eng. Comm.*, **13** [21] (2011) 6451–6456.
16. A. Ghule, N. Baskaran, R. Murugan, H. Chang, "Phase transformation studies of Na_3PO_4 by thermo Raman and conductivity measurements", *Solid State Ionics*, **161** [3] (2003) 291–299.
17. N. Gorodylova, P. Šulcová, M. Bosacka, I. Filipek, "DTA-TG and XRD study on the reaction between $ZrOCl_2 \cdot 8\,H_2O$ and $(NH_4)_2HPO_4$ for synthesis of ZrP_2O_7", *J. Therm. Anal. Calorim.*, **118** [2] (2014) 1095–1100.
18. R.C. Garvie, "The occurrence of metastable tetragonal zirconia as a crystallite size effect", *J. Phys. Chem.*, **69** [4] (1965) 1238–1243.
19. S.J. Milne, A.R. West, "Zr-doped Na_3PO_4: crystal chemistry, phase relations, and polymorphism", *J. Solid State Chem.*, **57** [2] (1985) 166–177.
20. Y.N. Xia, P.D. Yang, Y.G. Sun, Y. Wu, B. Mayers, B. Gates, Y. Yin, F. Kim, H. Yan, "One-dimensional nanostructures: synthesis, characterization, and applications", *Adv. Mater.*, **15** [5] (2003) 353–389.
21. M.A. Einarsrud, T. Grande, "1D oxide nanostructures from chemical solutions", *Chem. Soc. Rev.*, **43** [7] (2014) 2187–2199.